This is a repository copy of *Real-time monitoring of greenhouse gas emissions with tall chambers reveals diurnal N 2 O variation and increased emissions of CO 2 and N 2 O from miscanthus following compost addition*.

White Rose Research Online URL for this paper:
http://eprints.whiterose.ac.uk/152657/

Version: Published Version

GLOBAL CHANGE BIOLOGY
BIOENERGY   WILEY

Real-time monitoring of greenhouse gas emissions with tall chambers reveals diurnal N$_2$O variation and increased emissions of CO$_2$ and N$_2$O from *Miscanthus* following compost addition

J. Ben Keane[1,2] | Ross Morrison[3] | Niall P. McNamara[4] | Phil Ineson[1]

[1]Department of Biology, University of York, York, UK

[2]Department of Animal and Plant Sciences, The University of Sheffield, Sheffield, UK

[3]Centre for Ecology & Hydrology, Wallingford, UK

[4]Centre for Ecology & Hydrology, Lancaster Environment Centre, Lancaster, UK

Correspondence
J. Ben Keane, Department of Animal and Plant Sciences, The University of Sheffield, Alfred Denny Building, Western Bank, Sheffield S10 2TN 15, UK.
Email: ben.keane@sheffield.ac.uk

Abstract

Miscanthus x giganteus's efficacy as an energy crop relies on maintaining low greenhouse gas (GHG) emissions. As demand for *Miscanthus* is expected to rise to meet bioenergy targets, fertilizers and composts may be employed to increase yields, but will also increase GHG emissions. Manipulation experiments are vital to investigate the consequences of any fertilizer additions, but there is currently no way to measure whole-plant GHG fluxes from crops taller than 2.5 m, such as *Miscanthus*, at the experimental plot scale. We employed a unique combination of eddy covariance (EC), soil chambers and an entirely new automated chamber system, SkyBeam, to measure high frequency (ca. hourly) fluxes of carbon dioxide (CO$_2$), methane (CH$_4$) and nitrous oxide (N$_2$O) from a *Miscanthus* crop amended with green compost. Untreated controls were also monitored in a fully replicated experimental design. Net ecosystem exchange (NEE) of CO$_2$ was partitioned into soil respiration (R_s), gross primary productivity (GPP) and ecosystem respiration, and the crop was harvested to determine the effect of compost on crop productivity. Compost increased NEE emissions by 100% ($p < .05$), which was the result of a 20% increase of R_s ($p < .06$) and a 32% reduction in GPP ($p < .05$) and biomass of 37% ($p < .06$). Methane fluxes were small and unaffected by compost addition. N$_2$O emissions increased 34% under compost during an emission event; otherwise, fluxes were low and often negative, even under dry conditions. Diurnal variation in N$_2$O fluxes, with uptake during the day and emission at night was observed. These fluxes displayed a negative relationship with soil temperature and a hitherto undescribed diurnal temperature hysteresis. We conclude that compost addition negatively affected the productivity and environmental effects of *Miscanthus* cultivation during the first year following application.

KEYWORDS
automated chambers, bioenergy, diurnal, eddy covariance, greenhouse gases, *Miscanthus*, nitrous oxide, SkyBeam

1 | INTRODUCTION

To combat climate change, it may be necessary to use biomass to produce as much as a third of our future energy requirements (IPCC, 2014). The perennial C_4 grass *Miscanthus* (*Miscanthus x giganteus*) has been the subject of great interest (Clifton-Brown, Stampfl, & Jones, 2004; van der Weijde et al., 2013), due to its high productivity and relatively low nutrient requirements, particularly its low demand for nitrogen (N) fertilizer (St Clair, Hillier, & Smith, 2008), which it recycles during senescence over winter (Strullu, Cadoux, Preudhomme, Jeuffroy, & Beaudoin, 2011). It is expected that the uptake of *Miscanthus* cultivation across Europe will increase greatly over the coming years to meet energy needs, particularly if economic barriers are alleviated (Clifton-Brown et al., 2017). One way to improve economic viability is to increase productivity, and various studies have investigated the effect of fertilizer on *Miscanthus* yield, with mixed results. While some authors have reported no response (see Maughan et al., 2012; Teat, Neufeld, Gehl, & Gonzales, 2015), recently the balance of evidence suggests that fertilizer increases yields (Chen et al., 2019; Wang, Smyth, Crozier, Gehl, & Heitman, 2018; Xu, Gauder, Gruber, & Claupein, 2017). Emissions of the powerful greenhouse gas (GHG) nitrous oxide (N_2O), derived from N fertilizer, are the biggest source of GHGs from agriculture after livestock methane (CH_4; FAO, 2015), and the use of fertilizer and composts can also lead to increased soil respiration (R_s; Garcia-Delgado et al., 2018; Ozlu & Kumar, 2018) and CH_4 emissions (Fernandez-Luqueno et al., 2010; Thangarajan, Bolan, Tian, Naidu, & Kunhikrishnan, 2013), two other important components of a net GHG balance. Previous work has shown that GHG emissions, and especially N_2O fluxes, from *Miscanthus* are much lower than conventional crop rotations (Drewer, Finch, Lloyd, Baggs, & Skiba, 2012), and this is key to its viability as a bioenergy crop (Whitaker et al., 2018). Therefore, if it becomes common practice to apply fertilizer to energy crops, it may fundamentally change the GHG balance of energy crop production which is crucial to their purpose. It is long recognized that any potential increase in GHG emissions is factored into the overall GHG balance for cultivation of bioenergy feedstocks, and this demands robust measurements of GHG fluxes during the life cycle of the crop's cultivation.

Recent work suggests that N_2O has not been fully accounted for in previous *Miscanthus* GHG studies, with both conversion to *Miscanthus* (Holder et al., 2019) and reversion from *Miscanthus* (McCalmont et al., 2018) leading to increases in N_2O emissions. Furthermore, independent studies of GHG emissions from an established *Miscanthus* plantation in the United Kingdom have pointed to brief episodes of high N_2O emissions (Case, McNamara, Reay, & Whitaker, 2014; Drewer et al., 2012; Robertson et al., 2017); however, due to

the gaps between flux measurements, the frequency and magnitude of these singular emissions are not known. Previous investigations into the GHG emissions associated with *Miscanthus* production have generally relied on manual static chamber flux measurements (Drewer et al., 2012; Gauder, Butterbach-Bahl, Graeff-Honninger, Claupein, & Wiegel, 2012), with the greatest temporal resolution being biweekly (Oates et al., 2016). Furthermore, a failure to measure on a sub-daily basis potentially neglects important information regarding the diurnal variation in GHG fluxes, commonly seen in R_s (Bahn, Schmitt, Siegwolf, Richter, & Bruggemann, 2009; Yao et al., 2009; Yu et al., 2013), but also reported for fluxes of N_2O (Blackmer, Robbins, & Bremner, 1982; Das et al., 2012; Shurpali et al., 2016) and CH_4 (Hendriks, van Huissteden, & Dolman, 2010; Subke et al., 2018). Where automated chambers have been deployed to measure GHG fluxes from *Miscanthus* (Peyrard, Ferchaud, Mary, Grehan, & Leonard, 2017), measurements have not included vegetation due to the practicalities of building a chamber large enough to measure from a 3 m tall crop, disregarding the potential role that plants can play in promoting fluxes of N_2O (Ferch & Römheld, 2001; Pihlatie, Ambus, Rinne, Pilegaard, & Vesala, 2005) and CH_4 (Butterbach-Bahl, Kiese, & Liu, 2011; Rusch & Rennenberg, 1998).

The eddy covariance (EC) approach measures GHG fluxes at ecosystem scale, accounting for all the sources and sinks within its footprint and thus providing an estimate of the exchange of the gases of interest. Due to this, and the continuous data the technology yields, EC has become increasingly popular for quantifying GHG fluxes of carbon dioxide (CO_2) and CH_4 in particular. The EC approach has limitations, however, including topographical restrictions and difficulties measuring during stable atmospheric conditions at night, but perhaps the biggest drawback is its inability to resolve to the plot scale. Plot scale GHG measurements are vital for manipulative experiments, where the response of a system to a treatment may be followed in replication. Whilst whole-tree chambers have been built for flux measurements before (Mordacq, Ghashghaie, & Saugier, 1991), here we deployed a novel automated system, SkyBeam, which we believe is the first fully automated mobile chamber capable of measuring from tall (>2.5 m) vegetation. The clear chamber allowed photosynthesis to continue, with short chamber closure time ensuring that the crop was exposed to ambient conditions for as much of the study period as possible. Circulating the headspace gas through multiple analysers allowed the quantification of fluxes of CO_2, N_2O and CH_4 from a single chamber closure. This new approach allowed monitoring of N_2O, CO_2 and CH_4 from *Miscanthus* in near real-time, to explore the extent to which episodic emissions of GHG occurred.

Using a combination of SkyBeam, automated soil flux chambers and EC, we were able to conduct a fully replicated field experiment to investigate the effect of adding a green

compost to *Miscanthus x giganteus* on: (a) the frequency and magnitude of N_2O emissions events; (b) net exchange of CO_2, N_2O and CH_4; (c) R_s; and (d) crop productivity in the first year after application. Furthermore, the combination of techniques applied allowed investigation into the partitioning of carbon fluxes from NEE data to assess which elements of the C cycle would influence changes to the GHG balance following compost addition.

2 | MATERIALS AND METHODS

2.1 | Site description and compost experiment

All work was undertaken at a commercial farm in the east of the United Kingdom on a soil type of Beccles 1 association, fine silt over clay (described in detail by Drewer et al., 2012). The experiment was undertaken in an 11.5 ha field. The *Miscanthus* was a mature 7 year old stand which had not received any fertilizer for at least 2 years prior to this experimental work and the biomass was grown to supply nearby Drax power station in North Yorkshire, United Kingdom. Typically, *Miscanthus* emerges during May–June and grows rapidly until October, after which the biomass is left to senesce over winter and is harvested the following spring. However, following a disappointing harvest in 2012, the field was harrowed (ploughed to ca. 10 cm depth) in spring 2013 in an attempt to redistribute the rhizomes more evenly in order to improve yield, followed in July 2013 by an application of

green compost (46.6% C, 1.2% N, C:N = 38) which consisted of a range of decomposed woody material smaller than 5 cm to fine sawdust-like particles.

2.2 | Experimental design

The experimental area was selected following harvesting and subsequent harrowing of the *Miscanthus* crop in spring 2013. Emerging shoots across the field were surveyed using quadrats and, within a representative area, six plots (ca. 1.5 m × 2.5 m) were demarcated with each containing one landing base for the SkyBeam automated flux system and a 20 cm diameter collar for use with a Licor automated flux chamber (LI-8100, Licor; Figure 1). In July 2013, coinciding with the contractor's compost addition to the *Miscanthus* field, a subsample of the same compost was taken, well mixed and applied to the experimental plots by hand at the equivalent rate (4 T/ha). Plots were paired and one of each pair chosen at random to receive compost (+COMP), or to be maintained as a control (−COMP).

2.3 | SkyBeam automated chamber system

A full description of the SkyBeam (University of York) system can be found in Keane (2015). Briefly, it is an automated chamber system capable of measuring GHG fluxes from vegetation greater than 3 m tall (Figure 1). A single chamber is suspended from a 12 V powered trolley mounted on 10 m long aluminium gantry (height 6 m; Figure 1). Suspending
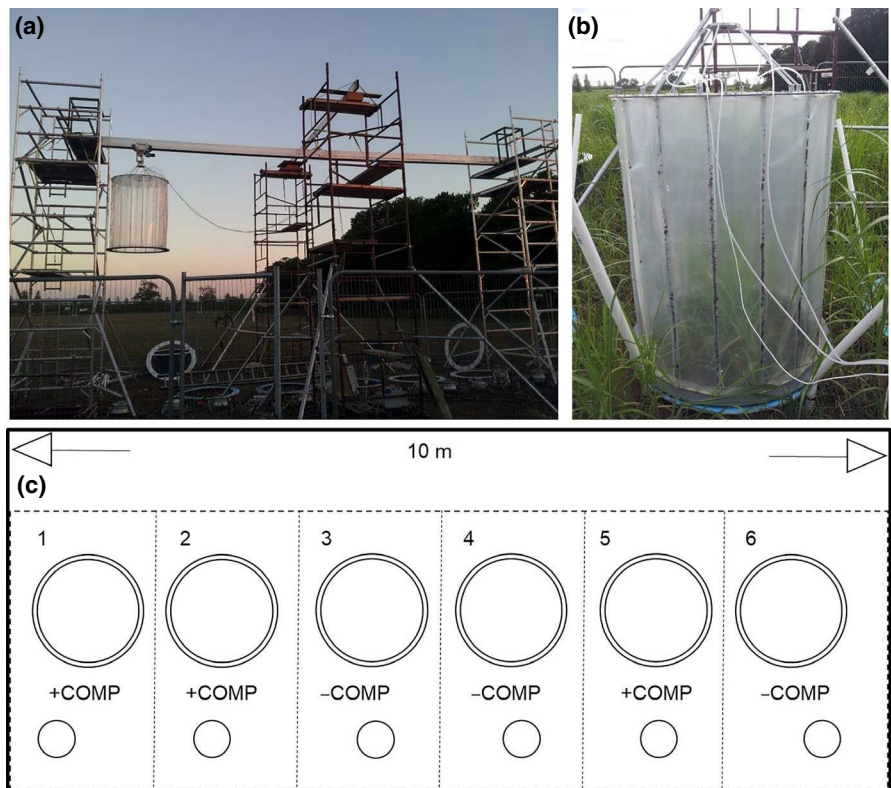

FIGURE 1 Construction of the SkyBeam system (a), showing the 6 m scaffolding towers and 10 m horizontal aluminium beam from which the chamber was suspended, with a motorized trolley providing lateral movement along a transect and landing bases on the ground. A chamber closure (b) during the early growing season 2013 showing the chamber enclosing *Miscanthus*. A schematic of the experimental layout (c) shows the plots with compost (+COMP) and controls (−COMP), where the large circles represent SkyBeam chamber bases and the smaller circles the automated chambers used for measurements of R_s

the chamber allowed repeated measurements to be taken from preselected points along a transect directly underneath the beam.

Each measurement consisted of lowering the chamber onto a landing base at one of the designated positions, before raising the chamber and moving to the next position. Automation of the system was achieved using a Licor infrared gas analyser (IRGA; LI-8100, Licor) to control the opening and closing and the length of closure of the large SkyBeam chamber in place of Licor-built automated soil flux chambers. The system was a dynamic closed-chamber system, where the headspace gas continually circulated via a 10 m length of polyethylene tubing (Bev-A-Line IV; Cole-Parmer) through the gas analysers, with the flow rate maintained at 2 L/min by the LI-8100.

The chamber (1 m internal diameter and 1.5 m in height) was a cage-like structure, with a circular clear Perspex roof sitting on top of a framework of vertical aluminium rods. A flat circular acrylic flange formed the chamber bottom, to which three concentric rings of closed cell rubber were fixed to ensure a gas tight seal with the landing based during chamber closure. The walls of the chamber were formed by stretching clear 720 gauge (180 μm) polythene (cat no. PM0026; First Tunnels), around the framework, sealed using fibreglass tape. Pressure inside the chamber was equalized with ambient pressure through the inclusion of a vent, after Xu et al. (2006). Landing bases consisted of flat circular flanges on which the bottom of the chamber sat during a measurement. Bases were positioned on the soil surface and packed with fine building sand to form a seal.

2.4 | GHG flux measurements

The SkyBeam chamber was deployed from June to December 2013. Measurement length was programmed as 10 min, with a delay of 2 min separating each measurement to allow the gas lines to purge. CO_2 fluxes from the SkyBeam system were calculated using the internal Licor software (Healy, Striegl, Russell, Hutchinson, & Livingston, 1996), with a dead band of 30 s to allow for mixing. The flux was calculated as a linear regression over 2 min, which was found to best describe the instantaneous flux at the time of closure.

CH_4 and N_2O fluxes were measured for two discrete campaigns of approximately 4 weeks each during the study: campaign 1 from 16 July to 12 August; campaign 2 from 6 September to 3 October. During these periods, two cavity ring down laser (CRD) analysers—a fast GHG analyser for CH_4 and an N_2O analyser (Los Gatos Research)—were incorporated into the SkyBeam assembly, drawing the headspace gas from the exhaust of the IRGA before returning it to the chamber. Both CRD analysers measured at 1 Hz, and fluxes were calculated as the linear regression of the change in concentration over time for a 240 s window following chamber closure. Fluxes were adjusted

for chamber volume, area and temperature, which were measured using a thermistor in the chamber headspace. Further adjustment was made to the CO_2 fluxes during daylight hours based on the light response curve to account for attenuation of light by the chamber material, after Heinemeyer, Gornall, Baxter, Huntley, and Ineson (2013). A detection limit was calculated for N_2O fluxes (Cowan et al., 2014) and is discussed further in Supporting Information. Fluxes of CO_2 measured using the SkyBeam chamber were discarded when $r^2 < .9$; using this as an indication of a successful chamber closure, N_2O and CH_4 fluxes which were significant ($p < .05$) were retained, and non-significant fluxes were considered to be zero.

Soil respiration measurements were made using opaque Licor automated chambers (Li-8100A; Licor) with a multiplexer (Department of Biology Workshops, University of York, York, UK). Chambers were placed over 20 cm diameter collars in the soil, and the collars were kept free of aboveground vegetation. Chambers were programmed to close for 3 min, with a 30 s dead band allowed for mixing, and fluxes were calculated as the linear regression of headspace CO_2 over the remaining closure period using Licor software.

2.5 | Eddy covariance measurements

Turbulent fluxes of sensible heat (H) and latent heat (H), and net ecosystem CO_2 exchange (NEE) were measured using an open-path EC system. Fluxes were computed using EddyPRO flux calculation software (LI-COR Biosciences Inc.). Raw (20 Hz) EC data were filtered for spikes (Mauder et al., 2013) and other implausible values (Vickers & Mahrt, 1997). Fluxes were computed as block averages using 30 min flux averaging intervals. The angle of attack correction (for Gill Instruments Ltd. sonic anemometers) and a two-dimensional coordinate rotation were applied to sonic anemometer data. Fluxes were corrected for low- and high-pass filtering (Moncrieff, Clement, Finnigan, & Meyers, 2004; Moncrieff et al., 1997) and H fluxes were corrected for humidity effects (Liu, Peters, & Foken, 2001; Schotanus, Nieuwstadt, & Debruin, 1983). Latent heat flux and CO_2 were adjusted for changes in air density related to temperature and humidity fluctuations (Webb, Pearman, & Leuning, 1980). Quality control procedures included statistical outlier removal (Papale et al., 2006) and rejection of data failing predetermined quality criteria (Foken & Leclerc, 2004; Ruppert, Mauder, Thomas, & Luers, 2006). Data gap-filling and partitioning of NEE into estimates of gross primary productivity (GPP) and total ecosystem respiration were performed according to Reichstein et al. (2005). Uncertainties were estimated as the standard deviation of measured (Finkelstein & Sims, 2001) and gap-filled (Wutzler, Reichstein, Moffat, & Migliavacca, 2018) flux data. The EC data are available at https://doi.org/10.5285/71e5b799-fc4d-4a44-8860-a5e358c807fd (Morrison, Rowe, Cooper, & McNamara, 2019).

2.6 | Environmental variables and harvest

Soil moisture and temperature were measured at 5 cm depth within each of the six experimental plots using SM200 moisture probes and ST1 temperature sensors, and logged as hourly averages on GP1 and DL2 dataloggers (Delta-T). Meteorological data (air temperature, solar radiation and relative humidity) were recorded as hourly averages using an on-site weather station (WP1; Delta-T). Solar radiation (W/m^2) was approximated to photon flux density of photosynthetically active radiation ($\mu mol\ m^{-2}\ s^{-1}$) using the equation (PPFD = 0.47 * solar radiation) from Pankaew, Milton, and Dash (2013). Rainfall data were retrieved from the Met Office MIDAS weather station ca. two miles from the site. Biomass was harvested by hand to coincide with the commercial harvest when the vegetation from each plot was cut at height analogous to mechanical harvesting in spring 2014 and oven-dried at 70°C until at constant weight.

2.7 | Data processing

All data analyses and manipulations were conducted in SAS 9.4 (SAS Institute). Cumulative fluxes for NEE were calculated for the period of continuous SkyBeam operation between July and October, and compared to EC fluxes over the same period. Cumulative N_2O and CH_4 fluxes were calculated for the two discrete measurement campaigns. The cumulative calculation was made using trapezoidal integration; repeated measures analysis of variance for treatment effects on daily mean fluxes was conducted using mixed effects models (SAS proc mixed), with chamber as a random effect. Similar to EC, SkyBeam NEE data were partitioned into ecosystem respiration (R_{eco}) and GPP following the method of Reichstein et al. (2005).

3 | RESULTS

3.1 | CO_2 fluxes

When the first measurements of NEE were collected using SkyBeam in mid-June, all fluxes were positive, indicating net emission of CO_2 to the atmosphere, but by the beginning of July, the crop had developed sufficiently to be a net sink of CO_2 during daylight hours (Figure 2). The magnitude of uptake increased through the summer, peaking at the beginning of September, where values measured were ca. $-17\ \mu mol\ m^{-2}\ s^{-1}$ ($-COMP$), $-8\ \mu mol\ m^{-2}\ s^{-1}$ ($+COMP$) and $-22\ \mu mol\ m^{-2}\ s^{-1}$ (Eddy covariance). Maximum release of CO_2 occurred during the night in late July, where values measured were ca. $10\ \mu mol\ m^{-2}\ s^{-1}$ (^-COMP and $+COMP$) and $11\ \mu mol\ m^{-2}\ s^{-1}$ (EC). R_s was low ($<5\ \mu mol\ m^{-2}\ s^{-1}$) at the start of July, but increased through the month (Figure 3). Fluxes declined through August and September except for a brief period around 14 September when maximum rates of R_s (ca. 7 and $10\ \mu mol\ m^{-2}\ s^{-1}$ for $-COMP$ and $+COMP$ respectively) were seen which coincided with rainfall, and this spike in R_s was reflected in a period of increased (more positive) NEE (Figure 3).

Daily mean NEE from the $+COMP$ treatment ($1.8\ \mu mol\ m^{-2}\ s^{-1}$) was more than 100% greater (more positive) than the $-COMP$ ($0.85\ \mu mol\ m^{-2}\ s^{-1}$, $F = 220.86$, $p < .001$) and this was reflected with a corresponding 20% increase in daily mean R_s from the $+COMP$ plots which approached significance ($F = 3.34$, $p < .07$; Figure 4). Although the magnitude of NEE measured with the EC system tended to be larger than the fluxes measured using SkyBeam, there was good agreement in the sign of the flux, and night-time values largely agreed (Figure 4). Daily mean flux fell within one standard error of the mean daily flux from the control plots (Figure 4). As the crop senesced through November into December, uptake reduced and night-time emissions also fell back to under $5\ \mu mol\ m^{-2}\ s^{-1}$. Over the study period,
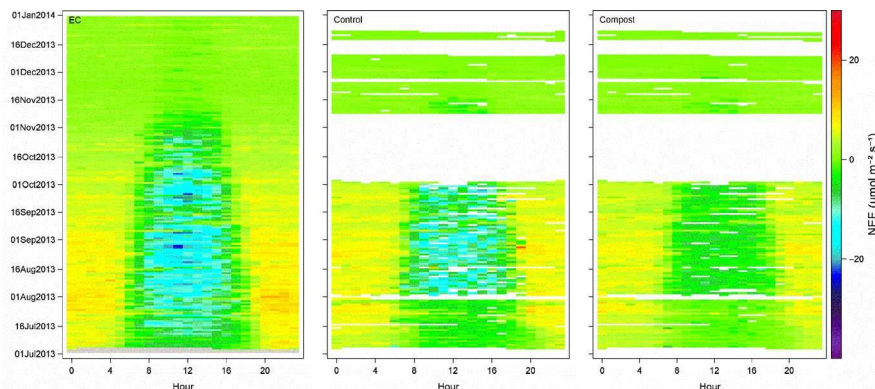

FIGURE 2 Net ecosystem exchange (NEE) of CO_2 measured from *Miscanthus x giganteus* using SkyBeam and eddy covariance (EC). EC data include measurements at field scale, which was treated with a green compost, SkyBeam was used to measure plots amended with the same compost and an untreated control. EC data are half hourly integrated measurements, SkyBeam are mean ($n = 3$, $\pm 1\ SE$) values of each measurement cycle (ca. hourly)
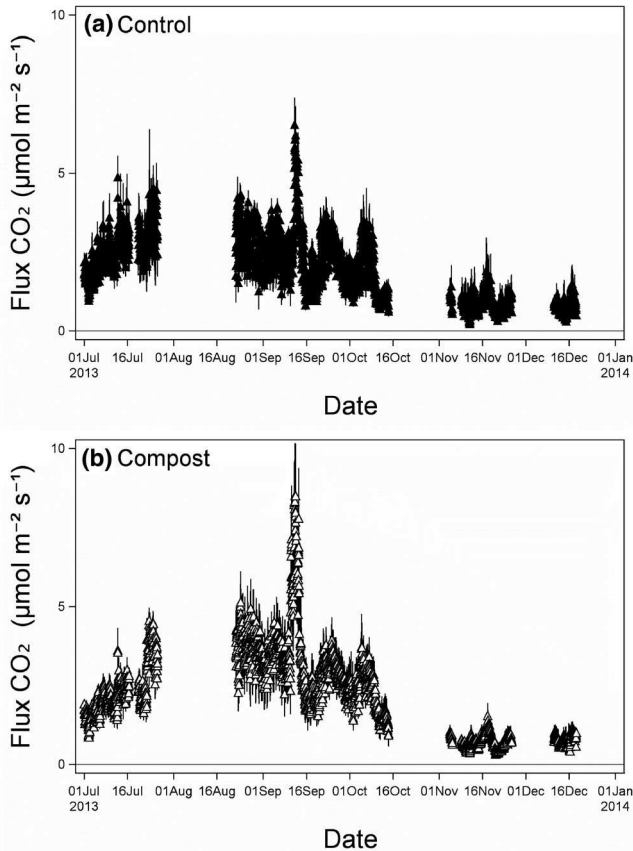
FIGURE 3 Soil respiration measured using Licor automatic chambers under *Miscanthus* from untreated controls (a) and compost addition (b) SkyBeam experimental plots from collars which excluded aboveground vegetation but included roots. Values shown are means ($n = 3$, ±1 SE)

GPP was 32% greater in −COMP plots (3.9 µmol m^{-2} s^{-1}) than from +COMP (2.6 µmol m^{-2} s^{-1}) plots ($F = 46.90$, $p < .001$; Figure 4), and the reduction in GPP and NEE under the compost treatment was reflected in 37% reduction in the

TABLE 1 Annual fluxes of C based on the average daily flux scaled up 1 July–31 December 2013. Values are the mean ± 1 SE ($n = 3$)

	Annual flux (Mg C ha/year)	
	Control	**Compost**
NEE	3.72 ± 1.83	7.90 ± 0.70
GPP	16.84 ± 1.67	11.46 ± 0.96
R_{eco}	20.50 ± 1.05	19.36 ± 1.21
R_{auto}	10.57 ± 2.18	8.42 ± 1.88
R_s	9.87 ± 1.25	10.92 ± 1.64

Abbreviations: GPP, gross primary productivity; NEE, net ecosystem exchange; R_{auto}, autotrophic respiration; R_{eco}, ecosystem respiration; R_s, soil respiration.
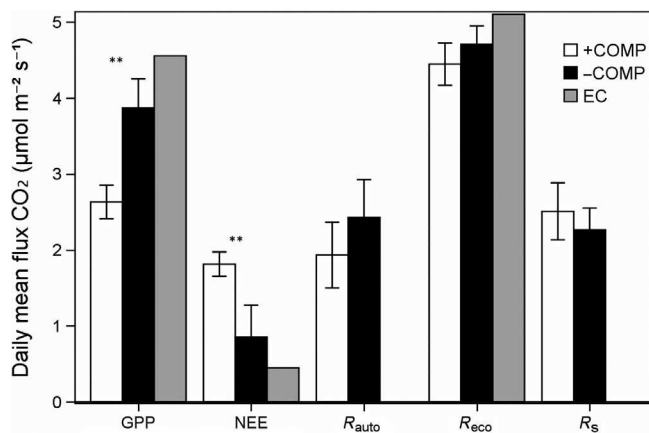

FIGURE 4 Daily mean carbon flux for 2013 growing season from SkyBeam experimental plots (+COMP, −COMP) and eddy covariance system (EC), partitioned into the various components: GPP, gross primary productivity; NEE, net ecosystem exchange; R_{auto}, autotrophic respiration; $R_{ec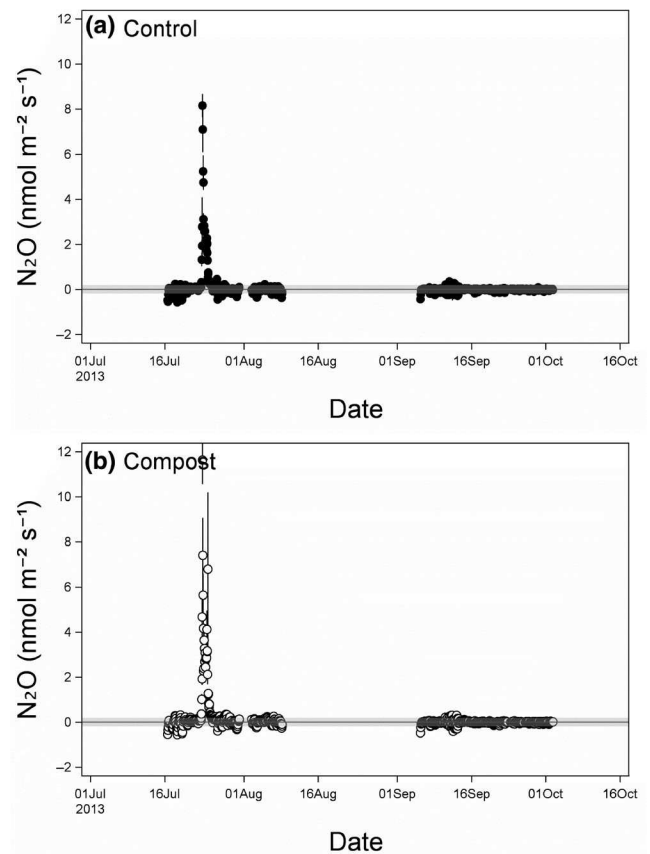o}$, ecosystem respiration; R_s, soil respiration. Data are means ($n = 3$, ±1 SEM), ** denotes significant differences ($p < .01$) between compost treatments. Positive values indicate a net release of CO_2 and negative values net sequestration

FIGURE 5 Flux of N_2O measured from *Miscanthus x giganteus* using SkyBeam amended with compost (b) and an untreated control (a). Values are mean ($n = 3$, ±1 SEM) values of each measurement cycle (ca. hourly). The calculated detection limit of SkyBeam, as outlined (Cowan et al., 2014; see Supporting Information), is represented by the horizontal grey band around the horizontal axis. Negative values indicate uptake and positive values release to the atmosphere

aboveground *Miscanthus* biomass harvested the following spring, of 2.02 ± 0.21 T/ha compared to 1.28 ± 0.19 T/ha from the compost ($F = 6.79$, $p < .06$). Annual fluxes of the C cycle are shown in Table 1.
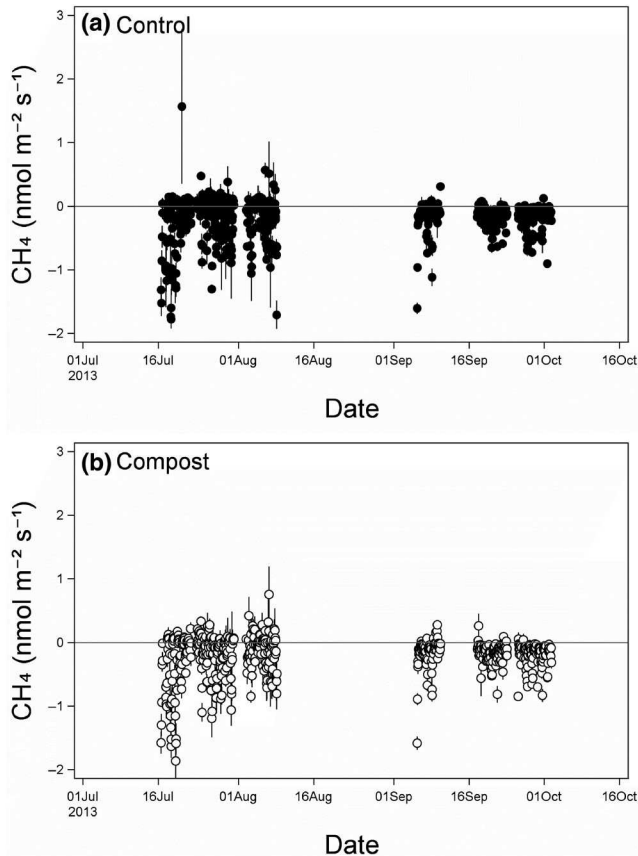

FIGURE 6 Flux of CH_4 measured from *Miscanthus x giganteus* using SkyBeam amended with compost (b) and an untreated control (a). Values are mean ($n = 3$, ± 1 *SEM*) values of each measurement cycle (ca. hourly). Negative values indicate uptake and positive values release to the atmosphere

3.2 | N_2O and CH_4 fluxes

The CH_4 fluxes were predominantly negative, indicating oxidation occurred in the soil (Figure 5). However, the magnitude of fluxes was small, so that CH_4 made a negligible contribution to the total GHG balance. N_2O fluxes were also small for the majority of the study, with 95% of fluxes in the range from 0.2 to -0.5 nmol m^{-2} s^{-1} (Figure 6), and over the entire study, there was no significant effect of compost addition on either the N_2O or CH_4 fluxes. However, there was a clear peak in N_2O emissions over 5 days, beginning on 22 July, where a maximum flux of 12 nmol m^{-2} s^{-1} was seen in the +COMP plots and 8 nmol m^{-2} s^{-1} from the −COMP plots. During this time, an average of $109.11 \pm 2.11\%$ and $94.70 \pm 12.25\%$ of the total N_2O flux from the first campaign was emitted from the −COMP and +COMP plots, respectively, with a significant ($F = 3.97$, $p < .05$) 34% increase in N_2O emissions from the +COMP treatment. This peak occurred following significant rainfall (8 mm) which was the first precipitation in over 4 weeks.

3.3 | Drivers of GHG fluxes

3.3.1 | CO_2 fluxes

The expected diurnal pattern of NEE was seen, with uptake during the day and net release at night. The relationship between NEE and PAR was well described by Michaelis–Menten response curves for fluxes measured using both EC and SkyBeam (Figure S1). For all but chambers 4 and 6, rates of CO_2 uptake were lower in SkyBeam plots than the entire EC footprint and the Pmax (maximum rate of GPP) values of the response curves were reflected in the biomass harvested from the chambers.
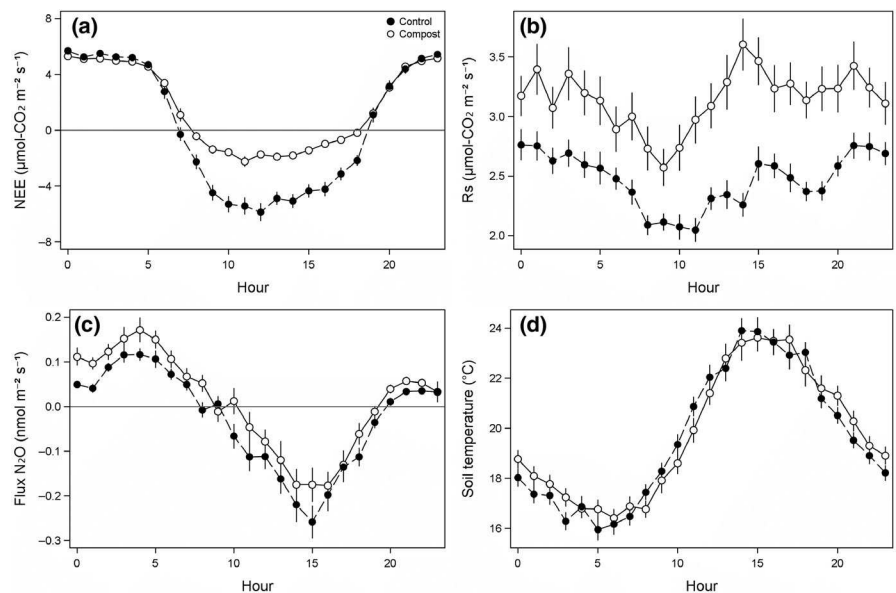

FIGURE 7 The mean diurnal pattern of NEE (a), soil respiration (b) and N_2O (c) and soil temperature (d) from SkyBeam experimental plots during Campaign 1 in 2013. Closed symbols denote control plots, open circles +COMP. Values shown are the averaged for plot ($n = 3$) and hour over the period
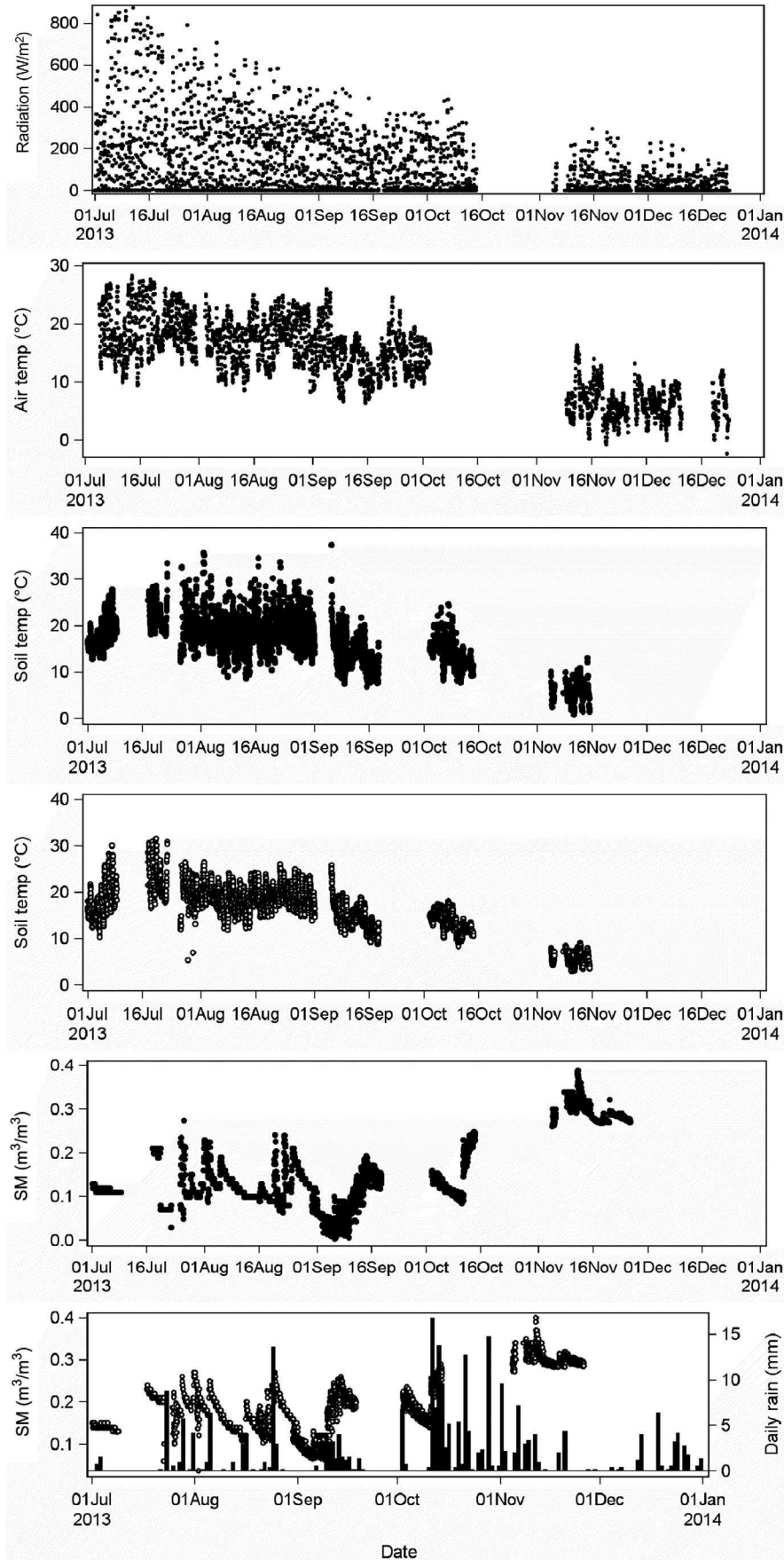
FIGURE 8 Meteorological variables measured during the field campaign in 2013

FIGURE 9 Mean hourly N_2O flux, measured using SkyBeam from *Miscanthus* from untreated controls (a) and with compost addition (b), against mean hourly soil temperature at 5 cm. Whilst there is a negative relationship between soil temperature and N_2O flux (as indicated by the linear regression and statistics included on the panel), there was also a clear hysteresis, which displayed an anticlockwise pattern. Each flux measurement is labelled with the hour
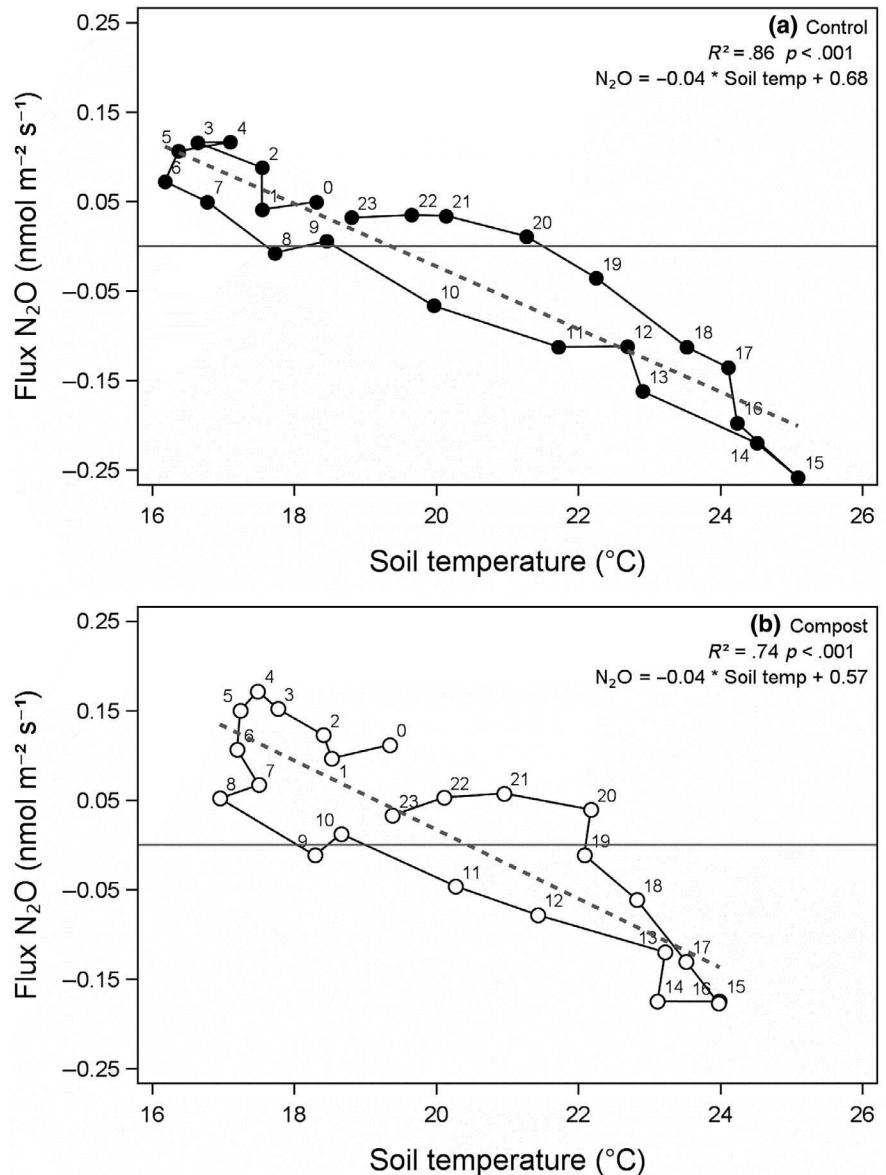
The diurnal pattern in R_s was not a simple sinusoidal form, but peaked twice during the day, once in the afternoon and once in the evening (Figure 7). This was reflected in the low correlation between R_s and soil temperature in both treatments ($r^2 = .13$ and $.11$, $p < .001$, −COMP and +COMP, respectively) across the whole period, though no other environmental variable explained more variation in fluxes.

3.3.2 | N_2O fluxes

During the emission event (22–25 July), N_2O fluxes were most closely related to the cumulative rainfall over the previous 24 hr for both the control and the compost treatments ($r^2 = .52$ and $.45$, $p < .001$ respectively). Between July and October, there was a significant increase in soil moisture at 5 cm depth under the +COMP treatment ($F = 7.65$, $p < .05$)

compared to the control, but there was no effect on soil temperature (Figure 8). Outside of this event, the most important predictor of N_2O flux during the first campaign was soil temperature, which displayed a clear negative relationship with N_2O flux ($r^2 = .26$ and $.16$, $p < .001$); furthermore, on a diurnal scale, the hourly N_2O fluxes showed a clear, anticlockwise hysteresis with soil temperature (Figure 9). The hysteresis is such that at similar temperatures, there was a switch in the direction of fluxes from positive to negative, with the greatest N_2O uptake coinciding with the first daily R_s peak (ca. 15.00).

4 | DISCUSSION

Using real-time monitoring of GHG emissions with tall chambers over *Miscanthus*, we have shown the importance of short-lived emissions' events with regard to the total GHG

flux and revealed a diurnal variation in N_2O emissions. We were also able to investigate the extent to which compost addition altered GHG emissions from this bioenergy crop.

4.1 | Effect of compost on N_2O emissions

The effect of compost addition was shown to be detrimental to several aspects of commercial *Miscanthus* production, most notably a reduction in the biomass produced. Whilst the productivity from both treatments was low, they were typical of year one harvest values for UK climatic conditions (McCalmont, McNamara, Donnison, Farrar, & Clifton-Brown, 2017), which perhaps reflects the disturbance caused by the harrowing of the field. Not only did the addition of compost to *Miscanthus* fail to improve productivity in our study but also it negatively affected the carbon balance of *Miscanthus* production by reducing GPP, whilst increasing NEE and R_s. Furthermore, compost addition also increased emissions of N_2O by more than a third compared to the non-composted control. Whilst the total emitted N_2O was small in terms of the GHG balance, any N_2O production during *Miscanthus* cultivation will reduce its efficacy as a CO_2 mitigation strategy. The increase in N_2O emissions measured under compost addition in our study was ca. 28 kg CO_2-eq/ha, and under annual application might lead to a further 513 kg CO_2-eq/ha (Table S1) being emitted over an 18 year life cycle of the crop (Robertson et al., 2017). The direct measurements of N_2O made in our study indicated that 0.13% of the compost was emitted as N_2O-N, which scales to an annual estimate of 0.47%, within the IPCC's emission factor of 1% (range of 0.3%–3%; De Klein et al., 2006).

4.2 | High N_2O emission event

Although the observed high flux event lasted only a few days following compost addition, its duration was slightly under 10% of the total time N_2O measurements were made during our study. If further high flux periods occurred at the same regularity outside of measurement campaigns, the annual budget would be greater than reported here. This flux event was characterized by a rapid increase in N_2O emissions following heavy rain (8 mm) marking the end of four dry weeks. Similar N_2O emissions events have been previously reported after rainfall (e.g. Breuer, Papen, & Butterbach-Bahl, 2000; Mummey, Smith, & Bolton, 1997; Saha et al., 2017), and we suggest that the driver of the event reported in this paper was that nitrate (NO_3) built up in the soil during the preceding dry weeks, which was rapidly denitrified as the soil became anaerobic following the rainfall, a process experimentally described elsewhere (Krichels, DeLucia, Sanford, Chee-Sanford, & Yang, 2019). This event reinforces the necessity to measure GHG fluxes at a temporal resolution appropriate to detect such emission events. The peak in N_2O emissions

seen here was equivalent to ca. 2000 μg m^{-2} hr^{-1}, which is more than ten times the magnitude of fluxes reported from *Miscanthus* in a long-term study at this site (Drewer et al., 2012) and approximately half the maximum rate seen at this farm following the addition of 120 kg N/ha ammonium nitrate fertilizer to oilseed rape (OSR, *Brassica napus* L.; Keane et al., 2018). While fluxes of a similar magnitude have been reported from unfertilized *Miscanthus* elsewhere (Guzman, Ussiri, & Lal, 2017), N_2O emissions from established *Miscanthus* plantations are widely thought to be much lower than those from conventional cropping (McCalmont, Hastings, et al., 2017).

4.3 | Uptake of N_2O and the diurnal variation of fluxes

A striking characteristic of the N_2O fluxes presented here was the diurnal pattern, particularly for the first N_2O campaign. Whilst diurnal patterns of N_2O emission have been seen several times before (e.g. Alves et al., 2012; Ryden, Lund, & Focht, 1978; Shurpali et al., 2016; Yamulki et al., 2001), and were very recently observed in OSR at the same farm (Keane et al., 2018), the diurnal variation reported by these authors was defined by a peak in emissions during the day and lower emissions during the night. The sole exception was reported by Shurpali et al. (2016), who saw higher emissions at night under N-limiting conditions. Of these studies, all but Keane et al. (2018) attribute the pattern to soil temperature, and to our knowledge, there are no reports of a transition between N_2O uptake during the day and production during the night.

The majority of N_2O uptake in soils is thought to be the result of complete denitrification of N_2O to dinitrogen (N_2) gas, which is a process that occurs in anoxic conditions, and therefore at high soil moisture content (Conen & Neftel, 2007). The negative fluxes presented here occurred at very low soil moisture content (<0.2 m^3/m^3). It has been suggested that soil microbes will reduce N_2O even in relatively dry (20% water-filled pore space) soils (Warneke, Macdonald, Macdonald, Sanderman, & Farrell, 2015), with negative fluxes even reported at 2% soil water content (Wu et al., 2013). Negative fluxes of N_2O have also been reported in dry and oxic vegetated soils under grasslands (Flechard, Neftel, Jocher, Ammann, & Fuhrer, 2005) and forestry (Goldberg & Gebauer, 2009). There is strong evidence that uptake in soils is a biological process (Warneke et al., 2015; Wu et al., 2013) and it has been demonstrated recently that, contrary to previous understanding, some obligate aerobic bacteria can reduce N_2O to N_2 (Park, Kim, & Yoon, 2017). It has largely been accepted that the consumption of N_2O by microbes is through its use as an electron acceptor, particularly when NO_3 in the soil is scarce (Flechard et al., 2005); in such conditions, denitrification by heterotrophic nitrifiers

might drive greater N_2O reduction than production, leading to a net negative flux. However, the specific aerobic microbial N_2O consumption pathway has not yet been confirmed, despite recent identification of novel N_2O-reducing organisms (Hallin, Philippot, Loffler, Sanford, & Jones, 2018). But laboratory work on several marine bacteria has shown that microbes possessing the *nifH* gene responsible for N_2 fixation can also use N_2O to assimilate N directly (Farias et al., 2013) in the presence of O_2, a process which is twice as energetically efficient as N_2 fixation and therefore may be preferable to such microbes. Stable isotope probing, using $^{15}N_2O$ to incubate a variety of aerated low-N soils has revealed the presence of ^{15}N in microbial organic compounds (J.E. Stockdale, C.B. Whitby, B. McKew, & P. Ineson, in preparation), suggesting that similar N_2O fixation may also occur in soils. It has been shown that *Miscanthus* rhizomes host N_2 fixers (Davis et al., 2010; Liu & Ludewig, 2019), which have been suggested as an explanation for its high N use efficiency and this could be a contributing factor to N_2O uptake seen here. Diurnal variation in *nifH* expression and N fixation has been demonstrated to be controlled by CO_2 concentrations (Stockel, Elvitigala, Liberton, & Pakrasi, 2013) and given that the highest daily rates of N_2O uptake presented here coincided with highest daily rates of R_s, it would suggest that N_2O consumption peaked when CO_2 concentration in the soil was greatest. Alternatively, if N_2O uptake was driven by heterotrophic nitrifier denitrification, this may have been stimulated by the arrival of C in the rhizosphere from photosynthate, which would also drive the first daily peak in R_s at around 15.00.

Given the presence of vegetation in the SkyBeam chamber, it should not be discounted that N_2O uptake was a plant-mediated process, or the interaction of the plant and soil microbes. It has previously been shown that maize (*Zea mays* L), a C_4 grass like *Miscanthus*, can absorb N_2O through stomata which it both metabolizes and stores (Grundmann, Lensi, & Chalamet, 1993). As diurnal maximum N_2O uptake coincided with peak GPP, it is possible that this was the cause of the pattern seen in our study. Positive plant-mediated fluxes of N_2O have been posited previously, where the N_2O is produced in the soil and transported to the atmosphere through the transpiration stream (Ferch & Römheld, 2001); if N_2O is being consumed at depth in the soil, it is perhaps possible that the reverse is true and that atmospheric N_2O is transported along a concentration gradient through the *Miscanthus*.

4.4 | Temperature hysteresis of N_2O flux

The negative relationship of N_2O fluxes with soil temperature in this study suggests that N_2O uptake increased with rising temperature. Mills, Dewhirst, Sowerby, Emmett, and Jones (2013) found a similar negative relationship between N_2O flux and soil temperature as reported here, even to the

extent that fluxes switched from positive to negative above 20°C, but that work was conducted on a podzol at field capacity, a contrast to the drier conditions at our study site. The situation is complicated as both uptake and emission occurred in the same location, with the balance altering throughout the day. The net flux is the sum of both of these processes, which may have different drivers. This is perhaps reflected in the diurnal hysteresis in the relationship between flux and soil temperature. Hystereses have been demonstrated several times between R_s and soil temperature (e.g. Phillips, Nickerson, Risk, & Bond, 2011; Riveros-Iregui et al., 2007; Zhang et al., 2015) and even under *Miscanthus* at the same study site (Keane & Ineson, 2017), but we believe that this is the first time temperature hysteresis on a diurnal scale has been reported for N_2O fluxes. Since it appears that increasing temperature stimulated greater uptake, the anticlockwise hysteresis presented here is analogous to a clockwise hysteresis in R_s fluxes, which has been suggested to be a consequence of thermal effects on gas diffusivity in soil (Zhang et al., 2015). The same authors did not consider that soil moisture fluctuations in the rooting zone were sufficiently large to be an important driver of hysteresis on a diurnal scale, and moisture levels in the bulk soil certainly did not vary so greatly over the course of the day to attribute N_2O uptake to this process here. As with the diurnal pattern of N_2O flux, we suggest that the temperature hysteresis may be driven by plant carbon; increasing soil temperature between 09.00 and 15.00 drives N_2O uptake in the soil, which declines with temperature until 17.00. The arrival of photosynthate to the rhizosphere could then supply C which stimulates heterotrophic denitrification and therefore N_2O production between ca. 20.00 and 09.00. Pulse labelling with ^{13}C in *Miscanthus* at this site has shown that C is available to soil microbes four hours after assimilation (Elias et al., 2017), and with highest rates of NEE seen from 11.00 to 15.00, photosynthate should start to arrive at the rhizosphere around 15.00. This coincided with the increase in N_2O fluxes, and the arrival of plant C to the soil late in the day might also explain why R_s remained above the daily average throughout the night time, despite coinciding with the lowest soil temperatures.

5 | CONCLUSION

The SkyBeam system performed well, producing CO_2 data which compared favourably with EC observations. The chamber system facilitated GHG flux measurements at the plot scale, enabling replicated manipulation experiments impossible with EC alone. Whilst large chambers have been built previously to measure gas exchange from over large vegetation (Mordacq et al., 1991), we have not found another automated flux system working at this scale for such

a continuous period. Automation of the system was vital to identify not only the diurnal characteristics of GHG fluxes but also to detect the short-lived burst of N_2O emissions between 22 and 26 July. Had a monthly or even weekly measurement schedule of manual measurements been conducted, it is likely that this event would have been missed.

Our study into the effects of compost addition on *Miscanthus* cultivation after harrowing identified negative effects on the GHG balance and crop productivity. This supports the notion that all farm interventions, across the life cycle of a crop, need to be considered for understanding the GHG balances of bioenergy crop cultivation. In this particular study, we have presented strong evidence that both cyclical and episodic events of N_2O can occur that impact on the net GHG balance of bioenergy systems. Our measured N_2O emissions in the context of reversion (McCalmont et al., 2018) and conversion (Holder et al., 2019) of bioenergy crops are relatively small, however, with other fertilizers and in other situations, such emissions may become tangible factors in GHG life cycle emissions. Fundamentally, there is a need for further investigation of the processes underlying N_2O uptake and emission in plants and soil, which is relevant to both fertilized and unfertilized bioenergy and food crops, to reduce uncertainties surrounding environmental benefits (Whitaker et al., 2018).

ORCID

J. Ben Keane [ID] https://orcid.org/0000-0001-7614-8018
Ross Morrison [ID] https://orcid.org/0000-0002-1847-3127

REFERENCES

Alves, B. J. R., Smith, K. A., Flores, R. A., Cardoso, A. S., Oliveira, W. R. D., Jantalia, C. P., … Boddey, R. M. (2012). Selection of the most suitable sampling time for static chambers for the estimation of daily mean N_2O flux from soils. *Soil Biology and Biochemistry*, *46*, 129–135. https://doi.org/10.1016/j.soilbio.2011.11.022

Bahn, M., Schmitt, M., Siegwolf, R., Richter, A., & Bruggemann, N. (2009). Does photosynthesis affect grassland soil-respired CO_2 and its carbon isotope composition on a diurnal timescale? *New Phytologist*, *182*(2), 451–460. https://doi.org/10.1111/j.1469-8137.2008.02755.x

Blackmer, A. M., Robbins, S. G., & Bremner, J. M. (1982). Diurnal variability in rate of emission of nitrous oxide from soils. *Soil Science Society of America Journal*, *46*(5), 937–942.

Breuer, L., Papen, H., & Butterbach-Bahl, K. (2000). N_2O emission from tropical forest soils of Australia. *Journal of Geophysical Research-Atmospheres*, *105*(D21), 26353–26367. https://doi.org/10.1029/2000jd900424

Butterbach-Bahl, K., Kiese, R., & Liu, C. Y. (2011). Measurements of biosphere-atmosphere exchange of CH_4 in terrestrial ecosystems. In A. C. Rosenzweig & S. W. Ragsdale (Eds.), *Methods in enzymology: Methods in methane metabolism, Vol 495, Pt B* (pp. 271–287). San Diego, CA: Elsevier Academic Press Inc.

Case, S. D. C., McNamara, N. P., Reay, D. S., & Whitaker, J. (2014). Can biochar reduce soil greenhouse gas emissions from a *Miscanthus* bioenergy crop? *Global Change Biology Bioenergy*, *6*(1), 76–89. https://doi.org/10.1111/gcbb.12052

Chen, H. H., Dai, Z. M., Jager, H. I., Wullschleger, S. D., Xu, J. M., & Schadt, C. W. (2019). Influences of nitrogen fertilization and climate regime on the above-ground biomass yields of *Miscanthus* and switchgrass: A meta-analysis. *Renewable and Sustainable Energy Reviews*, *108*, 303–311. https://doi.org/10.1016/j.rser.2019.03.037

Clifton-Brown, J., Hastings, A., Mos, M., McCalmont, J. P., Ashman, C., Awty-Carroll, D., … Flavell, R. (2017). Progress in upscaling *Miscanthus* biomass production for the European bio-economy with seed-based hybrids. *Global Change Biology Bioenergy*, *9*(1), 6–17. https://doi.org/10.1111/gcbb.12357

Clifton-Brown, J. C., Stampfl, P. F., & Jones, M. B. (2004). *Miscanthus* biomass production for energy in Europe and its potential contribution to decreasing fossil fuel carbon emissions. *Global Change Biology*, *10*(4), 509–518. https://doi.org/10.1111/j.1529-8817.2003.00749.x

Conen, F., & Neftel, A. (2007). Do increasingly depleted delta N-15 values of atmospheric N_2O indicate a decline in soil N_2O reduction? *Biogeochemistry*, *82*(3), 321–326. https://doi.org/10.1007/s10533-006-9066-y

Cowan, N. J., Famulari, D., Levy, P. E., Anderson, M., Reay, D. S., & Skiba, U. M. (2014). Investigating uptake of N_2O in agricultural soils using a high-precision dynamic chamber method. *Atmospheric Measurement Techniques*, *7*(12), 4455–4462. https://doi.org/10.5194/amt-7-4455-2014

Das, B. T., Hamonts, K., Moltchanova, E., Clough, T. J., Condron, L. M., Wakelin, S. A., & O'Callaghan, M. (2012). Influence of photosynthetically active radiation on diurnal N_2O emissions under ruminant urine patches. *New Zealand Journal of Agricultural Research*, *55*(4), 319–331. https://doi.org/10.1080/00288233.2012.697068

Davis, S. C., Parton, W. J., Dohleman, F. G., Smith, C. M., Del Grosso, S., Kent, A. D., & DeLucia, E. H. (2010). Comparative biogeochemical cycles of bioenergy crops reveal nitrogen-fixation and low greenhouse gas emissions in a *Miscanthus x giganteus* agroecosystem. *Ecosystems*, *13*(1), 144–156. https://doi.org/10.1007/s10021-009-9306-9

De Klein, C., Novoa, R. S. A., Ogle, S., Smith, K. A., Rochette, P., Wirth, T. C., … Walsh, M. (2006). N_2O emissions from managed soils, and CO_2 emissions from lime and urea application. *IPCC Guidelines for National Greenhouse Gas Inventories, Prepared by the National Greenhouse Gas Inventories Programme*, *4*, 1–54.

Drewer, J., Finch, J. W., Lloyd, C. R., Baggs, E. M., & Skiba, U. (2012). How do soil emissions of N_2O, CH_4 and CO_2 from perennial bioenergy crops differ from arable annual crops? *Global Change Biology Bioenergy*, *4*(4), 408–419. https://doi.org/10.1111/j.1757-1707.2011.01136.x

Elias, D. M. O., Rowe, R. L., Pereira, M. G., Stott, A. W., Barnes, C. J., Bending, G. D., & McNamara, N. P. (2017). Functional differences in the microbial processing of recent assimilates under two contrasting perennial bioenergy plantations. *Soil Biology and Biochemistry*, *114*, 248–262. https://doi.org/10.1016/j.soilbio.2017.07.026

FAO. (2015). Food and Agriculture Organization of the United Nations, FAOSTAT database. Retrieved from http://faostat3.fao.org/faostat-gateway/go/to/home/

Farias, L., Faundez, J., Fernandez, C., Cornejo, M., Sanhueza, S., & Carrasco, C. (2013). Biological N_2O fixation in the eastern South Pacific Ocean and marine cyanobacterial cultures. *PLoS ONE*, *8*(5), 12. https://doi.org/10.1371/journal.pone.0063956

Ferch, N. J., & Römheld, V. (2001). Release of water-dissolved nitrous oxide by plants: Does the transpiration water flow contribute to the emission of dissolved N_2O by sunflower? In W. J. Horst, M. K. Schenk, A. Bürkert, N. Claassen, H. Flessa, W. B. Frommer, H. Goldbach, H. W. Olfs, V. Römheld, B. Sattelmacher, U. Schmidhalter, S. Schubert, N. V. Wirén, & L. Wittenmayer (Eds.), *Plant nutrition: Food security and sustainability of agro-ecosystems through basic and applied research* (pp. 228–229). Dordrecht, Netherlands: Springer.

Fernandez-Luqueno, F., Reyes-Varela, V., Cervantes-Santiago, F., Gomez-Juarez, C., Santillan-Arias, A., & Dendooven, L. (2010). Emissions of carbon dioxide, methane and nitrous oxide from soil receiving urban wastewater for maize (*Zea mays* L.) cultivation. *Plant and Soil*, *331*(1–2), 203–215. https://doi.org/10.1007/s11104-009-0246-0

Finkelstein, P. L., & Sims, P. F. (2001). Sampling error in eddy correlation flux measurements. *Journal of Geophysical Research-Atmospheres*, *106*(D4), 3503–3509. https://doi.org/10.1029/2000jd900731

Flechard, C. R., Neftel, A., Jocher, M., Ammann, C., & Fuhrer, J. (2005). Bi-directional soil/atmosphere N_2O exchange over two mown grassland systems with contrasting management practices. *Global Change Biology*, *11*(12), 2114–2127. https://doi.org/10.1111/j.1365-2486.2005.01056.x

Foken, T., & Leclerc, M. Y. (2004). Methods and limitations in validation of footprint models. *Agricultural and Forest Meteorology*, *127*(3–4), 223–234. https://doi.org/10.1016/j.agrformet.2004.07.015

Garcia-Delgado, C., Barba, V., Marin-Benito, J. M., Igual, J. M., Sanchez-Martin, M. J., & Rodriguez-Cruz, M. S. (2018). Simultaneous application of two herbicides and green compost in a field experiment: Implications on soil microbial community. *Applied Soil Ecology*, *127*, 30–40. https://doi.org/10.1016/j.apsoil.2018.03.004

Gauder, M., Butterbach-Bahl, K., Graeff-Honninger, S., Claupein, W., & Wiegel, R. (2012). Soil-derived trace gas fluxes from different energy crops – Results from a field experiment in Southwest Germany. *Global Change Biology Bioenergy*, *4*(3), 289–301. https://doi.org/10.1111/j.1757-1707.2011.01135.x

Goldberg, S. D., & Gebauer, G. (2009). Drought turns a Central European Norway spruce forest soil from an N_2O source to a transient N_2O sink. *Global Change Biology*, *15*(4), 850–860. https://doi.org/10.1111/j.1365-2486.2008.01752.x

Grundmann, G. L., Lensi, R., & Chalamet, A. (1993). Delayed NH_3 and N_2O uptake by maize leaves. *New Phytologist*, *124*(2), 259–263. https://doi.org/10.1111/j.1469-8137.1993.tb03815.x

Guzman, J. G., Ussiri, D., & Lal, R. (2017). Greenhouse gas emissions following conversion of a reclaimed minesoil to bioenergy crop production. *Land Degradation & Development*, *28*(8), 2563–2573. https://doi.org/10.1002/ldr.2808

Hallin, S., Philippot, L., Loffler, F. E., Sanford, R. A., & Jones, C. M. (2018). Genomics and ecology of novel N_2O-reducing microorganisms. *Trends in Microbiology*, *26*(1), 43–55. https://doi.org/10.1016/j.tim.2017.07.003

Healy, R. W., Striegl, R. G., Russell, T. F., Hutchinson, G. L., & Livingston, G. P. (1996). Numerical evaluation of static-chamber measurements of soil-atmosphere gas exchange: Identification of physical processes. *Soil Science Society of America Journal*, *60*(3), 740–747. https://doi.org/10.2136/sssaj1996.03615995006000030009x

Heinemeyer, A., Gornall, J., Baxter, R., Huntley, B., & Ineson, P. (2013). Evaluating the carbon balance estimate from an automated ground-level flux chamber system in artificial grass mesocosms. *Ecology and Evolution*, *3*(15), 4998–5010. https://doi.org/10.1002/ece3.879

Hendriks, D. M. D., van Huissteden, J., & Dolman, A. J. (2010). Multitechnique assessment of spatial and temporal variability of methane fluxes in a peat meadow. *Agricultural and Forest Meteorology*, *150*(6), 757–774. https://doi.org/10.1016/j.agrformet.2009.06.017

Holder, A. J., McCalmont, J. P., Rowe, R., McNamara, N. P., Elias, D., & Donnison, I. S. (2019). Soil N_2O emissions with different reduced tillage methods during the establishment of *Miscanthus* in temperate grassland. *Global Change Biology Bioenergy*, *11*(3), 539–549. https://doi.org/10.1111/gcbb.12570

IPCC. (2014). *Climate Change 2014: Synthesis Report. Contribution of Working Groups I, II and III to the Fifth Assessment Report of the Intergovernmental Panel on Climate Change* [Core Writing Team, R. K. Pachauri & L. A. Meyer (Eds.)]. Geneva, Switzerland: IPCC.

Keane, J. B. (2015). *The development of novel technologies for the measurement of greenhouse gas fluxes from agricultural systems*. PhD thesis, University of York, UK.

Keane, J. B., & Ineson, P. (2017). Technical note: Differences in the diurnal pattern of soil respiration under adjacent *Miscanthus x giganteus* and barley crops reveal potential flaws in accepted sampling strategies. *Biogeosciences*, *14*(5), 1181–1187. https://doi.org/10.5194/bg-14-1181-2017

Keane, J. B., Ineson, P., Vallack, H. W., Blei, E., Bentley, M., Howarth, S., … Toet, S. (2018). Greenhouse gas emissions from the energy crop oilseed rape (*Brassica napus*); the role of photosynthetically active radiation in diurnal N_2O flux variation. *Global Change Biology Bioenergy*, *10*(5), 306–319. https://doi.org/10.1111/gcbb.12491

Krichels, A., DeLucia, E. H., Sanford, R., Chee-Sanford, J., & Yang, W. H. (2019). Historical soil drainage mediates the response of soil greenhouse gas emissions to intense precipitation events. *Biogeochemistry*, *142*(3), 425–442. https://doi.org/10.1007/s10533-019-00544-x

Liu, Y., & Ludewig, U. (2019). Nitrogen-dependent bacterial community shifts in root, rhizome and rhizosphere of nutrient-efficient *Miscanthus x giganteus* from long-term field trials. *Global Change Biology Bioenergy*, *14*, 1–14. https://doi.org/10.1111/gcbb.12634

Liu, H. P., Peters, G., & Foken, T. (2001). New equations for sonic temperature variance and buoyancy heat flux with an omnidirectional sonic anemometer. *Boundary-Layer Meteorology*, *100*(3), 459–468. https://doi.org/10.1023/a:1019207031397

Mauder, M., Cuntz, M., Drüe, C., Graf, A., Rebmann, C., Schmid, H. P., … Steinbrecher, R. (2013). A strategy for quality and

uncertainty assessment of long-term eddy-covariance measurements. *Agricultural and Forest Meteorology*, *169*, 122–135. https://doi.org/10.1016/j.agrformet.2012.09.006

Maughan, M., Bollero, G., Lee, D. K., Darmody, R., Bonos, S., Cortese, L., … Voigt, T. (2012). Miscanthus giganteus productivity: The effects of management in different environments. *Global Change Biology Bioenergy*, *4*(3), 253–265. https://doi.org/10.1111/j.1757-1707.2011.01144.x

McCalmont, J. P., Hastings, A., McNamara, N. P., Richter, G. M., Robson, P., Donnison, I. S., & Clifton-Brown, J. (2017). Environmental costs and benefits of growing *Miscanthus* for bioenergy in the UK. *Global Change Biology Bioenergy*, *9*(3), 489–507. https://doi.org/10.1111/gcbb.12294

McCalmont, J. P., McNamara, N. P., Donnison, I. S., Farrar, K., & Clifton-Brown, J. C. (2017). An interyear comparison of CO_2 flux and carbon budget at a commercial-scale land-use transition from semi-improved grassland to *Miscanthus x giganteus*. *Global Change Biology Bioenergy*, *9*(1), 229–245. https://doi.org/10.1111/gcbb.12323

McCalmont, J. P., Rowe, R., Elias, D., Whitaker, J., McNamara, N. P., & Donnison, I. S. (2018). Soil nitrous oxide flux following land-use reversion from *Miscanthus* and SRC willow to perennial ryegrass. *Global Change Biology Bioenergy*, *10*(12), 914–929. https://doi.org/10.1111/gcbb.12541

Mills, R. T. E., Dewhirst, N., Sowerby, A., Emmett, B. A., & Jones, D. L. (2013). Interactive effects of depth and temperature on CH_4 and N_2O flux in a shallow podzol. *Soil Biology & Biochemistry*, *62*, 1–4. https://doi.org/10.1016/j.soilbio.2013.03.003

Moncrieff, J. B., Clement, R., Finnigan, J. J., & Meyers, T. (2004). Averaging and de-trending. Handbook of Micrometeorology. In X. Lee, W. Massman, & B. Law (Eds.), *Averaging, detrending, and filtering of eddy covariance time series* (pp. 7–31). Dordrecht, The Netherlands: Springer.

Moncrieff, J. B., Massheder, J. M., de Bruin, H., Elbers, J., Friborg, T., Heusinkveld, B., … Verhoef, A. (1997). A system to measure surface fluxes of momentum, sensible heat, water vapour and carbon dioxide. *Journal of Hydrology*, *188*(1–4), 589–611. https://doi.org/10.1016/S0022-1694(96)03194-0

Mordacq, L., Ghashghaie, J., & Saugier, B. (1991). A simple field method for measuring the gas exchange of small trees. *Functional Ecology*, *5*(4), 572–576. https://doi.org/10.2307/2389640

Morrison, R., Rowe, R., Cooper, H. C., & McNamara, N. P. (2019). Eddy covariance measurements of carbon dioxide, energy and water fluxes at a commercial *Miscanthus x giganteus* plantation, Lincolnshire, UK, 2013 to 2017. NERC Environmental Information Data Centre, https://doi.org/10.5285/71e5b799-fc4d-4a44-8860-a5e358c807fd

Mummey, D. L., Smith, J. L., & Bolton, H. (1997). Small-scale spatial and temporal variability of N_2O flux from a shrub-steppe ecosystem. *Soil Biology and Biochemistry*, *29*(11–12), 1699–1706. https://doi.org/10.1016/s0038-0717(97)00077-1

Oates, L. G., Duncan, D. S., Gelfand, I., Millar, N., Robertson, G. P., & Jackson, R. D. (2016). Nitrous oxide emissions during establishment of eight alternative cellulosic bioenergy cropping systems in the North Central United States. *Global Change Biology Bioenergy*, *8*(3), 539–549. https://doi.org/10.1111/gcbb.12268

Ozlu, E., & Kumar, S. (2018). Response of surface GHG fluxes to long-term manure and inorganic fertilizer application in corn and soybean rotation. *Science of the Total Environment*, *626*, 817–825. https://doi.org/10.1016/j.scitotenv.2018.01.120

Pankaew, P., Milton, E. J., & Dash, J. (2013). Estimating hourly variation in photosynthetically active radiation across the UK using MSG SEVIRI data. Paper presented at the 35th International Symposium on Remote Sensing of Environment (ISRSE35), Inst Remote Sensing & Digital Earth, Beijing, Peoples R China.

Papale, D., Reichstein, M., Aubinet, M., Canfora, E., Bernhofer, C., Kutsch, W., … Yakir, D. (2006). Towards a standardized processing of net ecosystem exchange measured with eddy covariance technique: Algorithms and uncertainty estimation. *Biogeosciences*, *3*(4), 571–583. https://doi.org/10.5194/bg-3-571-2006

Park, D., Kim, H., & Yoon, S. (2017). Nitrous oxide reduction by an obligate aerobic bacterium, *Gemmatimonas aurantiaca* strain T-27. *Applied and Environmental Microbiology*, *83*(12), e00502-17. https://doi.org/10.1128/aem.00502-17

Peyrard, C., Ferchaud, F., Mary, B., Grehan, E., & Leonard, J. (2017). Management practices of *Miscanthus x giganteus* strongly influence soil properties and N_2O emissions over the long term. *Bioenergy Research*, *10*(1), 208–224. https://doi.org/10.1007/s12155-016-9796-1

Phillips, C. L., Nickerson, N., Risk, D., & Bond, B. J. (2011). Interpreting diel hysteresis between soil respiration and temperature. *Global Change Biology*, *17*(1), 515–527. https://doi.org/10.1111/j.1365-2486.2010.02250.x

Pihlatie, M., Ambus, P., Rinne, J., Pilegaard, K., & Vesala, T. (2005). Plant-mediated nitrous oxide emissions from beech (*Fagus sylvatica*) leaves. *New Phytologist*, *168*(1), 93–98. https://doi.org/10.1111/j.1469-8137.2005.01542.x

Reichstein, M., Falge, E., Baldocchi, D., Papale, D., Aubinet, M., Berbigier, P., … Valentini, R. (2005). On the separation of net ecosystem exchange into assimilation and ecosystem respiration: Review and improved algorithm. *Global Change Biology*, *11*(9), 1424–1439. https://doi.org/10.1111/j.1365-2486.2005.001002.x

Riveros-Iregui, D. A., Emanuel, R. E., Muth, D. J., McGlynn, B. L., Epstein, H. E., Welsch, D. L., … Wraith, J. M. (2007). Diurnal hysteresis between soil CO_2 and soil temperature is controlled by soil water content. *Geophysical Research Letters*, *34*(17), 5. https://doi.org/10.1029/2007gl030938

Robertson, A. D., Whitaker, J., Morrison, R., Davies, C. A., Smith, P., & McNamara, N. P. (2017). A *Miscanthus* plantation can be carbon neutral without increasing soil carbon stocks. *Global Change Biology Bioenergy*, *9*(3), 645–661. https://doi.org/10.1111/gcbb.12397

Ruppert, J., Mauder, M., Thomas, C., & Luers, J. (2006). Innovative gap-filling strategy for annual SUMS of CO_2 net ecosystem exchange. *Agricultural and Forest Meteorology*, *138*(1–4), 5–18. https://doi.org/10.1016/j.agrformet.2006.03.003

Rusch, H., & Rennenberg, H. (1998). Black alder (*Alnus glutinosa* (L.) Gaertn.) trees mediate methane and nitrous oxide emission from the soil to the atmosphere. *Plant and Soil*, *201*(1), 1–7. https://doi.org/10.1023/a:1004331521059

Ryden, J. C., Lund, L. J., & Focht, D. D. (1978). Direct in-field measurement of nitrous oxide from soils. *Soil Science Society of America Journal*, *42*(5), 731–737. https://doi.org/10.2136/sssaj1978.03615995004200050015x

Saha, D., Rau, B. M., Kaye, J. P., Montes, F., Adler, P. R., & Kemanian, A. R. (2017). Landscape control of nitrous oxide emissions during the transition from conservation reserve program to perennial grasses for bioenergy. *Global Change Biology Bioenergy*, *9*(4), 783–795. https://doi.org/10.1111/gcbb.12395

Schotanus, P., Nieuwstadt, F. T. M., & Debruin, H. A. R. (1983). Temperature measurement with a sonic anemometer and its application to heat and moisture fluxes. *Boundary-Layer Meteorology*, *26*(1), 81–93. https://doi.org/10.1007/bf00164332

Shurpali, N. J., Rannik, Ü., Jokinen, S., Lind, S., Biasi, C., Mammarella, I., … Martikainen, P. J. (2016). Neglecting diurnal variations leads to uncertainties in terrestrial nitrous oxide emissions. *Scientific Reports*, *6*, 9. https://doi.org/10.1038/srep25739

St Clair, S., Hillier, J., & Smith, P. (2008). Estimating the pre-harvest greenhouse gas costs of energy crop production. *Biomass & Bioenergy*, *32*(5), 442–452. https://doi.org/10.1016/j.biombioe.2007.11.001

Stockel, J., Elvitigala, T. R., Liberton, M., & Pakrasi, H. B. (2013). Carbon availability affects diurnally controlled processes and cell morphology of cyanothece 51142. *PLoS ONE*, *8*(2), 10. https://doi.org/10.1371/journal.pone.0056887

Strullu, L. S. L., Cadoux, S., Preudhomme, M., Jeuffroy, M. H., & Beaudoin, N. (2011). Biomass production and nitrogen accumulation and remobilisation by *Miscanthus x giganteus* as influenced by nitrogen stocks in belowground organs. *Field Crops Research*, *121*(3), 381–391. https://doi.org/10.1016/j.fcr.2011.01.005

Subke, J. A., Moody, C. S., Hill, T. C., Voke, N., Toet, S., Ineson, P., & Teh, Y. (2018). Rhizosphere activity and atmospheric methane concentrations drive variations of methane fluxes in a temperate forest soil. *Soil Biology and Biochemistry*, *116*, 323–332. https://doi.org/10.1016/j.soilbio.2017.10.037

Teat, A. L., Neufeld, H. S., Gehl, R. J., & Gonzales, E. (2015). Growth and yield of Miscanthus x giganteus grown in fertilized and biochar-amended soils in the western North Carolina mountains. *Castanea*, *80*(1), 45–58. https://doi.org/10.2179/14-021r1

Thangarajan, R., Bolan, N. S., Tian, G. L., Naidu, R., & Kunhikrishnan, A. (2013). Role of organic amendment application on greenhouse gas emission from soil. *Science of the Total Environment*, *465*, 72–96. https://doi.org/10.1016/j.scitotenv.2013.01.031

van der Weijde, T., Kamei, C. L. A., Torres, A. F., Vermerris, W., Dolstra, O., Visser, R. G. F., & Trindade, L. M. (2013). The potential of C4 grasses for cellulosic biofuel production. *Frontiers in Plant Science*, *4*, 18. https://doi.org/10.3389/fpls.2013.00107

Vickers, D., & Mahrt, L. (1997). Fetch limited drag coefficients. *Boundary-Layer Meteorology*, *85*(1), 53–79. https://doi.org/10.1023/a:1000472623187

Wang, Z., Smyth, T. J., Crozier, C. R., Gehl, R. J., & Heitman, A. J. (2018). Yield and nitrogen removal of bioenergy grasses as influenced by nitrogen rate and harvest management in the coastal plain region of North Carolina. *Bioenergy Research*, *11*(1), 44–53. https://doi.org/10.1007/s12155-017-9876-x

Warneke, S., Macdonald, B. C. T., Macdonald, L. M., Sanderman, J., & Farrell, M. (2015). Abiotic dissolution and biological uptake of nitrous oxide in Mediterranean woodland and pasture soil. *Soil Biology and Biochemistry*, *82*, 62–64. https://doi.org/10.1016/j.soilbio.2014.12.014

Webb, E. K., Pearman, G. I., & Leuning, R. (1980). Correction of flux measurements for density effects due to heat and water-vapor transfer. *Quarterly Journal of the Royal Meteorological Society*, *106*(447), 85–100. https://doi.org/10.1002/qj.49710644707

Whitaker, J., Field, J. L., Bernacchi, C. J., Cerri, C. E. P., Ceulemans, R., Davies, C. A., … McNamara, N. P. (2018). Consensus, uncertainties and challenges for perennial bioenergy crops and land use. *Global Change Biology Bioenergy*, *10*(3), 150–164. https://doi.org/10.1111/gcbb.12488

Wu, D. M., Dong, W. X., Oenema, O., Wang, Y. Y., Trebs, I., & Hu, C. S. (2013). N₂O consumption by low-nitrogen soil and its regulation by water and oxygen. *Soil Biology and Biochemistry*, *60*, 165–172. https://doi.org/10.1016/j.soilbio.2013.01.028

Wutzler, T., Reichstein, M., Moffat, A. M., & Migliavacca, M. (2018). REddyProc: Post Processing of (Half-)Hourly Eddy-Covariance Measurements. R package version 1.1.5. Retrieved from https://CRAN.R-project.org/package=REddyProc

Xu, J., Gauder, M., Gruber, S., & Claupein, W. (2017). Yields of annual and perennial energy crops in a 12-year field trial. *Agronomy Journal*, *109*(3), 811–821. https://doi.org/10.2134/agronj2015.0501

Xu, L. K., Furtaw, M. D., Madsen, R. A., Garcia, R. L., Anderson, D. J., & McDermitt, D. K. (2006). On maintaining pressure equilibrium between a soil CO_2 flux chamber and the ambient air. *Journal of Geophysical Research-Atmospheres*, *111*(D8). https://doi.org/10.1029/2005JD006435

Yamulki, S., Toyoda, S., Yoshida, N., Veldkamp, E., Grant, B., & Bol, R. (2001). Diurnal fluxes and the isotopomer ratios of N_2O in a temperate grassland following urine amendment. *Rapid Communications in Mass Spectrometry*, *15*(15), 1263–1269. https://doi.org/10.1002/rcm.352

Yao, Z., Zheng, X., Xie, B., Liu, C., Mei, B., Dong, H., … Zhu, J. (2009). Comparison of manual and automated chambers for field measurements of N_2O, CH_4, CO_2 fluxes from cultivated land. *Atmospheric Environment*, *43*(11), 1888–1896. https://doi.org/10.1016/j.atmosenv.2008.12.031

Yu, L., Wang, H., Wang, G., Song, W., Huang, Y., Li, S.-G., … He, J.-S. (2013). A comparison of methane emission measurements using eddy covariance and manual and automated chamber-based techniques in Tibetan Plateau alpine wetland. *Environmental Pollution*, *181*, 81–90. https://doi.org/10.1016/j.envpol.2013.06.018

Zhang, Q., Katul, G. G., Oren, R., Daly, E., Manzoni, S., & Yang, D. W. (2015). The hysteresis response of soil CO_2 concentration and soil respiration to soil temperature. *Journal of Geophysical Research-Biogeosciences*, *120*(8), 1605–1618. https://doi.org/10.1002/2015jg003047

SUPPORTING INFORMATION

Additional supporting information may be found online in the Supporting Information section at the end of the article.